Наносистеми, наноматеріали, нанотехнології
Nanosistemi, Nanomateriali, Nanotehnologii
2021, т. 19, № 3, сс. 571–584

PACS numbers: 62.20.D-, 62.20.mm, 62.20.Qp, 62.25.Mn, 68.37.Hk, 81.40.Np, 83.60.Uv

Measurement of the Fracture Toughness and Mechanical Properties of Hydroxyapatite Using Vickers Indentation Technique

Mohsin A. Aswad

Department of Ceramics Engineering and Building Materials,
Faculty of Materials Engineering,
University of Babylon,
P.O. Box 4, Babylon, Iraq

The fracture toughness is a good asset that identifies a one of the important properties, namely, a brittleness of the hydroxyapatite material and the fracture strength. The applied load and the crack geometry are independent values for measuring the fracture toughness by using Vickers indentation technique. The kind of cracks observed in the hydroxyapatite sample is median–radial cracks at different ranges of applied loads using Vickers indentation method. The scanning electron microscope is used to observe and measure the crack length and visualize the crack tip and its development. The residual stress on the hydroxyapatite sample surface is identified from measuring fracture toughness, which is affected by small subcritical cracks, which are created under loading. The scanning electron microscope is used in this technique for showing the crack tip with high quality as well as crack profile and this process, which give a high accurate for calculating the fracture toughness. The mechanical properties of the hydroxyapatite samples are measured. Young's modulus and Poisson's ratio are measured using ultrasonic method and are used for calculation of the accuracy fracture-toughness values, and hardness is measured using Vickers indentation. Vickers crack opening displacement is measured from the mechanical properties (fracture toughness and Young's modulus) and the crack length, which give a good predication for measuring fracture toughness of the hydroxyapatite sample.

В'язкість руйнування є хорошим активом, який ідентифікує одну з важливих властивостей, а саме, крихкість гідроксиапатитного матеріялу та міцність на перелом. Прикладене навантаження та геометрія тріщин є незалежними значеннями для міряння в'язкости руйнування за допомогою техніки визначення твердости удавлюванням за Віккерсом. Вид тріщин, що спостерігаються в зразку гідроксиапатиту, — це серединно-радіяльні тріщини за різних діяпазонів прикладних наван-

тажень методом визначення твердости удавлюванням за Віккерсом. Сканувальний електронний мікроскоп використовується для спостереження і міряння довжини тріщини та візуалізації кінчика тріщини і її розвитку. Залишкове навантаження на поверхню гідроксиапатиту визначається міряннням в'язкости руйнування, на яку впливають невеликі підкритичні тріщини, які створюються за навантаження. Сканувальний електронний мікроскоп використовується в цій техніці для відображення кінчика тріщини з високою якістю, а також профілю тріщини та цього процесу, які дають високу точність для розрахунку в'язкости руйнування. Міряються механічні властивості зразків гідроксиапатиту. Модуль Юнґа та Пуассонове співвідношення міряються за допомогою ультразвукової методи та використовуються для розрахунку значень точности в'язкости руйнування, а твердість міряється за допомогою удавлювання за Віккерсом. Зміщення кінців (розкриття) тріщини за Віккерсом міряється за механічними властивостями (за в'язкістю перелому та модулем Юнґа) і довжиною тріщини, які дають хороший предикат для міряння в'язкости руйнування зразка гідроксиапатиту.

Key words: hydroxyapatite, Vickers indentation method, mechanical properties, fracture toughness, Vickers crack opening displacement.

Ключові слова: гідроксиапатит, метод удавлювання за Віккерсом, механічні властивості, в'язкість руйнування, розкриття тріщини за Віккерсом.

(Received 28 September, 2020)

1. INTRODUCTION

The bioceramics materials has a low fracture strength and it was identified by fracture toughness or called critical stress intensity factor in mode I (opening mode) of the bioceramic materials [1, 2]. For measuring fracture toughness, there are different types of methods for identified and calculating fracture toughness. One of most techniques for measuring fracture toughness uses notches for creating initial cracks. There is different method for measuring fracture toughness using notches for example single edge notch beam, chevron notch beam, and the Vickers indentation [3–5]. The indentation technique was used to measure K_{IC} depending on the kind of the materials, for example, ceramic materials, bioceramics [6–8].

There are many advantages for using Vickers indentation, for example, starting materials, simple equipment, and the sample finishing for this technique is fast and easy. The fracture toughness was measured using indentation technique directly by measuring the cracks length, which initiated after applied indenter on the sample surface [9–12].

Vickers indentation technique is not fracture the initial-cracked

sample and this technique related to the impression indenter on the finished sample surface [13, 14]. The area beneath of the indenter was deformed plastically and created the cracks at the four corners of the indent and then measuring the crack length. Dependences on the Vickers load, crack length, Young's modulus, hardness, and the size of indentation diagonal are used for calculating the fracture toughness [13].

Fracture toughness is resistance of the materials to develop the crack propagation. The microstructure of the ceramic materials is affected by the voids and pores on the samples surface and these defects are influence on the material resistance to the fracture. The profile of the defects in the ceramic materials takes into explanation, which used in the Griffith equations [15–17].

The fracture toughness was assessed by using the Vickers indentation technique, and the crack length measured directly from the indent corner. This method obtained attention for using in biomaterials to calculate K_{IC}. The cracks beneath the indent were created due to elastic plastic behaviour, which had given the type of the crack in this materials and this type is radial–median cracks because the tensile strength after unloading, and the fracture toughness equation as shown below [18, 19]:

$$K_{IC} = \alpha\left(\frac{E}{H}\right)^{1/2}\frac{P}{c^{3/2}}. \qquad (1)$$

This fracture toughness is according to the Anstis's equation on the Young's modulus, hardness, crack length, Vickers applied load. α is the constant for calibration and depends on the kind of cracks; for the radial–median crack, the value for this constant is 0.016 [18, 19].

There are four kinds of cracks initiated, which depend on the materials as shown in Fig. 1. Figure 1, *a* shows the radial crack, which diffuses from the regions close to the edges of the indent and spread down. Figure 1, *b* shows the median cracks; this kind of crack spread from the loading direction under the elastic–plastic zone as circular form. Figure 1, *c* shows the redial–median crack; this kind of crack

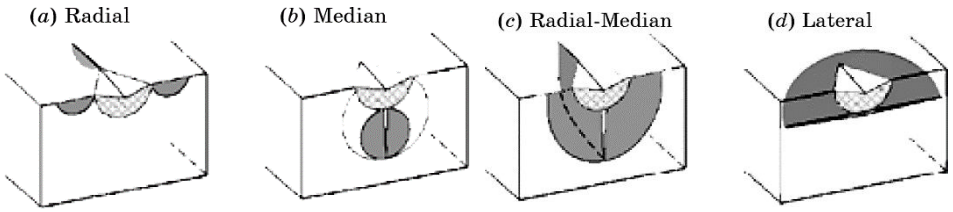

Fig. 1. The types of cracks, which initiated through applied Vickers load; the hatched area show the plastic regions [20].

diffuses beneath the indent and merge with the cracks at the corner of the indent to form this crack. Figure 1, *d* shows the last type of kind of cracks and is called lateral crack, which is parallel to the indenter surface after unloading and may cause chipping [17, 20].

The purpose of this paper is to use Vickers indentation technique to measure the fracture toughness of the local hydroxyapatite material. In addition, using method to identify the kind of cracks, they were radial–median cracks. Mechanical properties of the local hydroxyapatite materials were studied, for example, hardness, Young's modulus, and Poisson's ratio by using ultrasonic method. The aim of this paper to obtain the high-accuracy values of fracture toughness and using Vickers indentation with low cost, which used for the hydroxyapatite materials used in different applications.

2. EXPERIMENTAL WORK

2.1. Sample Preparation

The hydroxyapatite powders were supplied form the local market in Iraq. The powders of hydroxyapatite were mixed with poly-vinyl-alcohol at 2% weight for binding. The method was used for compaction the sample is semi-dry process with dimensions 15×8×4 mm for Vickers indentation. The samples were compacted under applied pressure of about 140 MPa and sintered at firing temperature of 1200°C. Then, the samples for indentation process were prepared by using grinding and polishing by diamond paste.

2.2. The Indentation Method

The technique was used for measuring the fracture toughness of hydroxyapatite sample by Vickers indentation using diamond pyramid tester. After applied Vickers load, which leads to showing the impressions of the indenter on the sample surface, then using optical microscope to observe the crack tip and crack length.

The cracks on the upper hydroxyapatite surface were shown by using this method as shown in Fig. 2. The applied Vickers loads of 2.9 N, 4.9 N, and 9.8 N were used in this process, the period of indentation was 10 sec, and the number on indents for each load was 4 indents.

2.3. Calculation of Mechanical Properties

The Young's modulus and Poisson's ratio were measured by using ultrasonic device CSI type CCT-4 at the Polymer Department Engineering in Materials Engineering, University of Babylon. The number of

Fig. 2. The impressions and crack on the hydroxyapatite sample under Vickers load of 9.8 N.

specimens, which were used for calculating the mechanical properties, was three samples used for this test having dimensions in diameter of 10 mm and height of 45 mm. The Young's modulus and Poisson's ratio were calculated by using Eqs. (2) and (3) [21]:

$$\nu = 1 - \frac{1}{2 - 2\left(\frac{C_s}{C_l}\right)^2}, \tag{2}$$

$$E = 2\rho C_s^2 (1 + \nu), \tag{3}$$

where C_l is velocity of longitudinal sound wave, C_s is velocity of shear sound wave, ρ is the specimen density, E is Young's modulus, and ν is Poisson's ratio.

2.4. Fracture Toughens

Vickers indentation technique was used for measuring the fracture toughness of the hydroxyapatite sample under Vickers loads of 2.9 N, 4.9 N, 9.8 N, and there are 4 readings for each loads. Anstis's equation is used to calculate the fracture toughness as shown in Eq. (4) [19]:

$$K_{1C} = 0.016\left(\frac{E}{H}\right)^{1/2} \frac{P}{c^{3/2}}, \tag{4}$$

where E—Young's modulus, H—the projected hardness number as shown below, P—the Vickers load, c—the radial crack length.

The kind of cracks observed on the hydroxyapatite sample was radial–median cracks, which are represented by crack length c, which is

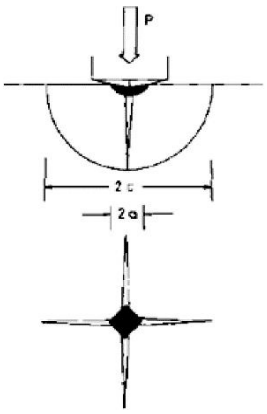

Fig. 3. Schematics of the indentation technique with kind of cracks [19].

used in the fracture toughness equation as shown in Fig. 3. The crack length was measured from the centre of the indent to the crack tip. Figure 3 represents the Vickers indentation and shows the Vickers load, P, the crack length, c, and the plastic of impression, a. The hardness, H, is measured by using simple analysis as shown in Eq. (4) [19]:

$$H = \frac{P}{\alpha_o a^2}, \tag{4}$$

where α_o—Vickers indenters constant ($\alpha_o = 2$), a—the half-diagonal of impression.

2.5. Test of Vickers Crack Opening Displacement

Irwin's equation was found relationship between the critical stress intensity factor K_{1C}, crack opening displacement $u(r)$, and the type of crack. This equation was used to evaluate the fracture toughness of the ceramic materials.

Crack opening displacement was measured using different method, for example, atomic force microscope and scanning electron microscope, but Fett has used analytical equation depending on the mechanical properties and crack length for measuring it as shown in Eq. (5) [18]:

$$u(r) = \frac{K_{tip}}{E'} \sqrt{\frac{8(c-r)}{\pi}}, \; E' = \frac{E}{1-\nu^2}, \tag{5}$$

where K_{tip} is the critical stress intensity factor, $u(r)$ is the crack opening displacement, r is the distance of the contact area, and c is the

crack length, E' is the modulus of the plane strain.

3. RESULTS AND DISCUSSION

3.1. Vickers Indentation

With increasing Vickers load through Vickers indentation, there is observation within the propagation of the cracks around the indent. At low forces, the indent starts with no cracks in the hardness impression, and, after increasing Vickers load, there four cracks begin at the corners of the indent, and the cracks continued underneath the impression.

The hydroxyapatite sample surface was prepared for observing the Vickers indent and cracks profile under optical microscope, which was used to identify the accurate values for the crack lengths. The curvature of the hydroxyapatite sample was small according to the Vickers indent. The kind of the cracks was radial–median cracks, which continued beneath the impression to the end of the crack tip, and they not clear sometimes, which needed high magnification technique. For avoiding the chipping onto sample surface, the Vickers load was applied to create cracks, and they developed to $c \geq 2a$.

3.2. Cracks Observation

The radial–median of cracks and crack length were shown clearly on the hydroxyapatite sample by painting the sample surface with thin film of the ink material. The sample surface with indentation was examined by using scanning electron microscope for observing the whole area of the Vickers test (plastic deformed area and cracks) as shown in Fig. 4, *a*. Figure 4, *a* on the right-hand side shows expanded region of the crack with red hidden area showing the crack opening after unloading; Figure 4, *b* shows the whole crack length, which is measured for calculating fracture toughness, but the image on the right-hand side shows the crack tip at high magnification in the hydroxyapatite samples.

The kind of the cracks created on the hydroxyapatite surface after applied load as identified in Fig. 5 were redial–median cracks developed radially from indent region. These kinds of cracks were diffused beneath the Vickers indent after sample preparation.

The Vickers technique was affected and limited to kind of materials, which performed their indent response, for example, materials with coarse grain size, monocrystalline ones, and soft ceramics. The kind of cracks was correlated with the ceramic materials nature and the profile of the cracks. Crack length was measured from the centre of the indent

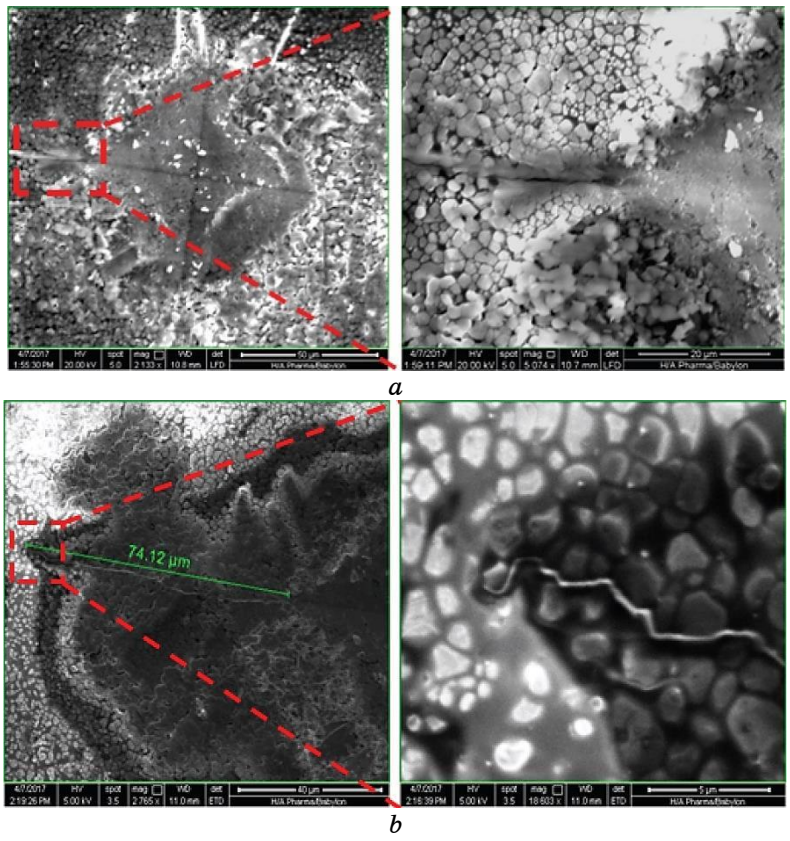

Fig. 4. *a*) The Vickers indent with create the crack on the edge of the indent and then magnify the red hidden region to observe the crack opening at Vickers loads of 9.8 N; *b*) the whole crack length and the hidden red region shows the crack tip with high magnification at Vickers loads of 9.8 N.

to the end of the crack tip by using scanning electron microscope. The type of the cracks was identified from removing the indent as shown in Fig. 5. The cracks diffused beneath the Vickers indent to form the radial–median crack or half-penny crack on the sample surface developed elsewhere other cracks to plastic deformed region due to the residual stresses at the indent, the influence of the other kinds of cracks may be neglected [18].

Figure 6 shows the relationship between the crack length and applied load; the crack was developed with increasing the applied load.

Figure 7 shows the relationship between the crack length–diagonal of indent, c/a versus the Vickers load. The c/a ratio decrease with increasing the applied load using Vickers indentation due to increasing diagonal size at 9.8 N, which is closed to the crack length.

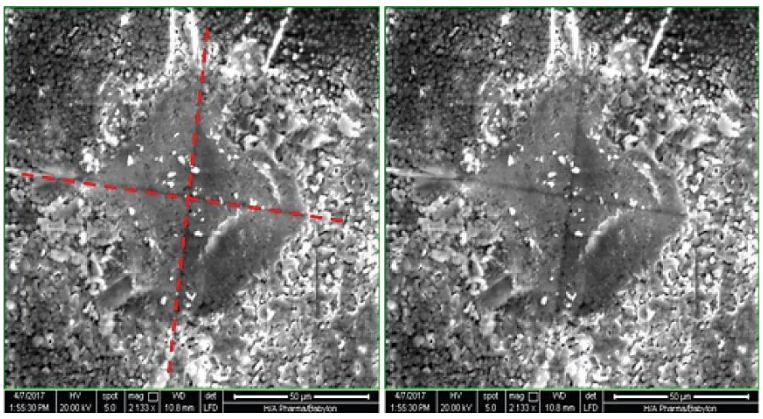

Fig. 5. The radial–median cracks on the hydroxyapatite surface and the red hidden line shows the cracks continued beneath the Vickers indent to the end of the crack tip at Vickers load of 9.8 N.

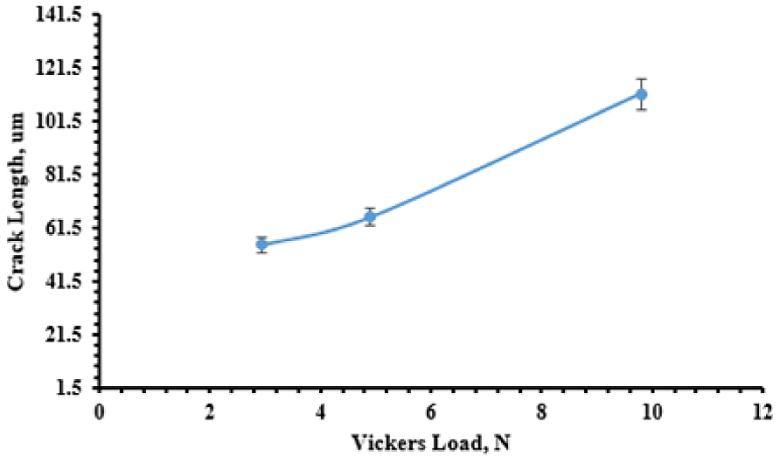

Fig. 6. The crack development with increasing the applied load of the hydroxyapatite sample.

3.3. Mechanical Properties: Young's Modulus *E* and Poisson's Ratio ν

The Young's modulus and Poisson's ratio were measured of the hydroxyapatite sample using ultrasonic technique as shown in Table 1. Increasing in the mechanical properties, K_{IC} and H, due to the increasing of the hydroxyapatite densification after sintering with high temperature of 1200°C, which enhanced the sample density and decreased in the sample porosity, as shown in scanning electron microscope images. These factors plays important role to improve the mechanical

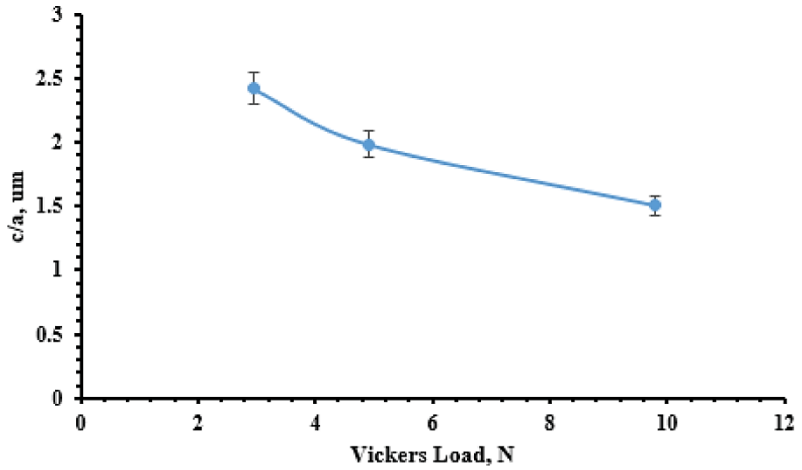

Fig. 7. The relationship between the c/a ratios against the Vickers load of the hydroxyapatite sample.

TABLE 1. The mechanical properties and the Vickers load as a function of the $P/c^{3/2}$ for the hydroxyapatite sample.

Vickers load, N	No. of indentations	a, μm	c, μm	H, GPa	E, GPa	ν	K_{IC}, MPa·m$^{1/2}$
2.94	4	22.75	55.10	1.96	104	0.33	$7.38 \cdot 10^{-1}$
4.9	4	33	65.55	2.107	104	0.33	$8.40 \cdot 10^{-1}$
9.8	4	74	111.5	3.528	104	0.33	$1.04 \cdot 10^{+01}$

properties.

Figure 8 shows the relationship between the Vickers hardness and applied load. The hardness increase with increasing load due to the indent and the crack length and tip were very clear at 9.8 N. The standard deviations was presented by using error bars and it calculate for a lowest four samples for each Vickers load and the values for error bars are small to observe in this figure.

3.4. Fracture Toughness

The quantity of the fracture toughness was measured after the transmitting the impression sample to the optical technique to observe the subcritical cracks. The relationship between the fracture toughness against applied Vickers load as shown in Table 1 and Fig. 9. The data in this figure was plotted depending on the Anstis's equation as mentioned in experimental section and the fracture toughness values were

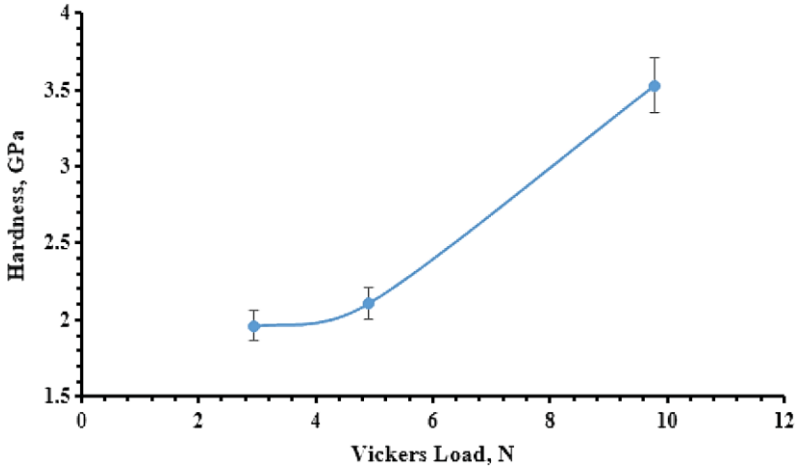

Fig. 8. The relationship between the hardness and Vickers load of the hydroxyapatite sample.

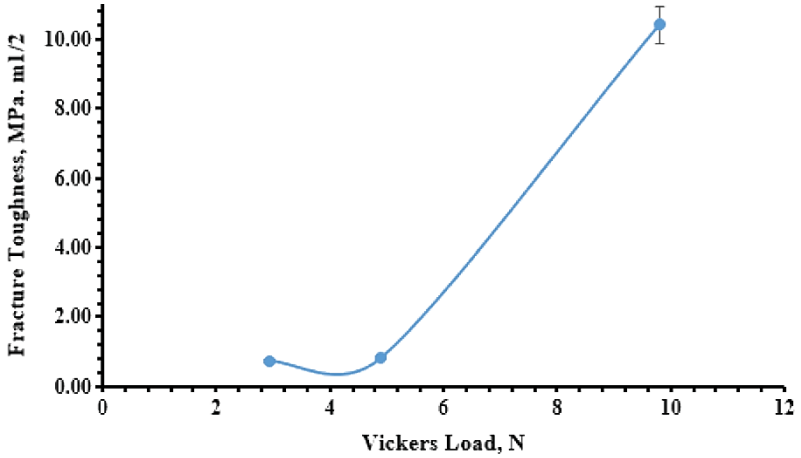

Fig. 9. The fracture toughness of the hydroxyapatite sample at different applied Vickers load.

effectively change according to applied load and with measuring the crack length. The fracture toughness increase with increasing crack length at Vickers load is of 9.8 N due to the measuring the crack length is clear and perfect as shown in scanning electron microscope images.

The simplicity and economy of the Vickers indentation technique versus of the accuracy of this method can be adopt to measure the fracture toughness of the ceramic materials. In addition, the materials properties, loading rate, crack length, Vickers load are a function of

the development in crack extension as shown in Fig. 6 [22]. Anstis's equation was used to calculate the fracture toughness for radial–median crack size as shown in Table 1 [19]. The development in the crack propagation is maximum influence on the fracture toughness values as shown in Fig. 6. The indentation Vickers method offers vision to the conception for the fracture toughness at the level of the cracks, which were created using Vickers load and shown under scanning electron microscope.

The uncertainty in the relationship between the Young's modulus to hardness were un-significant and the fracture toughness was effected by the elastic (E) and plastic (H) parameters, and those parameters are not known. The fracture toughness was related with crack length, when increasing crack length leads to increase the fracture toughness. The reasons for this relation related to adhesion loads at the surfaces of the crack, and these forces increases the K_{IC} and the effects of friction. Another reason is the subcritical cracks and branching of cracks, which caused to increase the fracture toughness [22]. The cracks branching and secondary cracks play important role in toughening mechanisms to dissipate the crack energy and improving the fracture toughness.

3.5. Vickers Crack Opening Displacement

The Vickers crack opening displacement was related to the mechanical properties (Young's modulus, Poisson's ratio, and fracture toughness) and the crack length, which initiated using Vickers indentation of the hydroxyapatite sample as shown in Table 2. There is good point for using VCOD; this method did not need to calibrate for using the VCOD equation. Another point for using the VCOD technique, this method not needs hardness values for measuring it. This method was a good method for measuring fracture toughness for ceramic materials [18].

Figure 10 shows the relationship between the Vickers loads against the Vickers crack opening displacement for hydroxyapatite sample. The VCOD increase with increasing the applied load due to the crack length and indent were clear and perfect for measuring the crack length and diagonal of crack at Vickers load is of 9.8 N.

TABLE 2. The relationship between the mechanical properties and Vickers crack opening displacement.

Vickers load, N	a, μm	c, μm	E, GPa	ν	E', GPa	K_{IC}, MPa·m$^{1/2}$	VCOD, μm
2.94	22.75	55.10	104	0.33	117	$7.38 \cdot 10^{-01}$	0.269
4.9	33	65.55	104	0.33	117	$8.40 \cdot 10^{-01}$	0.297
9.8	74	111.5	104	0.33	117	$1.04 \cdot 10^{+01}$	4.246

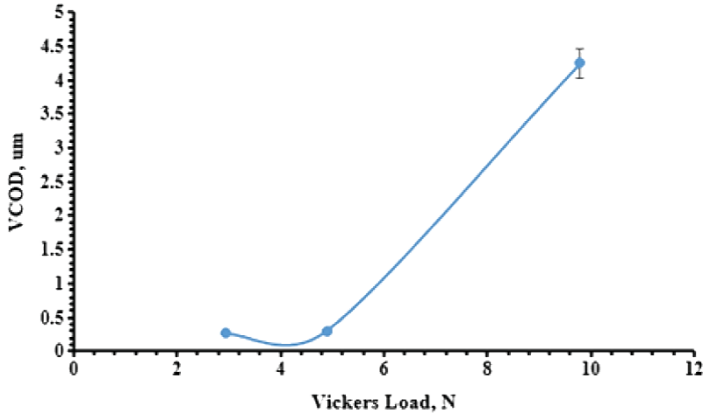

Fig. 10. The relationship between the Vickers load and Vickers crack opening displacement of the hydroxyapatite sample.

4. CONCLUSIONS

The crack tip and development in the crack propagation was observed using scanning electron microscope which they initiated using Vickers load.

The mechanical properties, Young's modulus and Poisson's ratio, were measured using ultrasonic method and the hardness was measured using Vickers indentation of the hydroxyapatite samples, and the accuracy value at 9.8 N is of 3.528 GPa.

The kind of the cracks were observed in the hydroxyapatite sample was radial–median cracks that means the cracks are diffused underneath the indent to the crack tip.

Vickers indentation method was economy, sufficient sensitivity, simplicity, and optimization for measuring fracture toughness in the hydroxyapatite samples and the accuracy value is of 11.04 MPa·$m^{1/2}$ and load is of 9.8 N.

The Vickers crack opening displacement was matched with the fracture toughness and that means COD is one the factor for measuring and predication of the fracture toughness values.

REFERENCES

1. A. Moradkhani, H. Baharvandi, and A. Naserifar, *Journal of the Korean Ceramic Society*, **56**, No. 1: 37 (2019); https://doi.org/10.4191/kcers.2019.56.1.01
2. E. S. Elshazly, S. M. El-Hout, and M. E. Ali, *J. Mater. Sci. Technol.*, **27**, No. 4: 332 (2011); https://doi.org/10.1016/S1005-0302(11)60070-4
3. K. Matsui, T. Yamakawa, M. Uehara, N. Enomoto, and J. Hojo, *J. Am. Ceram. Soc.*, **91**, No. 6: 1888 (2008); https://doi.org/10.1111/j.1551-

2916.2008.02350.x
4. M. Guazzato, M. Albakry, S. P. Ringer, and M. V. Swain, *Dent. Mater.*, **20**, No. 5: 4449 (2004); doi:10.1016/j.dental.2003.05.002
5. F. Egilmez, G. Ergun, I. C. Nagas, P. K. Vallittu, and L. V. Lassila, *J. Mech. Behave. Biomed. Mater.*, **37**: 78 (2014); doi:10.1016/j.jmbbm.2014.05.013
6. E. Camposilvan, F. G. Marro, A. Mestra, and M. Anglada, *Acta Biomater.*, **17**: 36 (2015).
7. M. M. Renjo, L. Ćurković, S. Štefančić, and D. Ćorić, *Dent. Mater.*, **30**, No. 12: 371 (2014).
8. K. Harada, A. Shinya, D. Yokoyama, and A. Shinya, *J. Prosthodont. Res.*, **57**, No. 2: 82 (2013).
9. G. K. Pereira, A. B. Venturini, T. Silvestri, K. S. Dapieve, A. F. Montagner, F. Z. Soares, and L. F. Valandro, *J. Mech. Behav. Biomed. Mater.*, **55**: 151 (2015); https://doi.org/10.1016/j.jmbbm.2015.10.017
10. A. Kailer and S. Marc, *Dent. Mater.*, **32**, No. 10: 1256 (2016).
11. A. Moradkhani, H. Baharvandi, M. Tajdari, H. Latifi, and J. Martikainen, *J. Adv. Ceram.*, **2**: 87 (2013); https://doi.org/10.1007/s40145-013-0047-z
12. A. Samodurova, A. Kocjan, M. V. Swain, and T. Kosmač, *Acta Biomater.*, **11**: 477 (2015).
13. G. D. Quinn, *Ceramic Engineering and Science Proceedings* (Eds. Rajan Tandon, Andrew Wereszczak, and Edgar Lara-Curzio) (2006), Ch. 5; https://doi.org/10.1002/9780470291313.ch5
14. G. D. Quinn, K. Xu, J. A. Salem, and J. J. Swab, *Fracture Mechanics of Glasses and Ceramics*, **14**: 499 (2005).
15. I. Hervas, A. Montagne, A. V. Gorp, M. Bentoumi, A. Thuault, and A. Iost, *Ceramics International*, **42**, No. 11: 12740 (2016); https://doi.org/10.1016/j.ceramint.2016.05.030
16. M. Barlet, J. M. Delaye, T. Charpentier, M. Gennisson, D. Bonamy, T. Rouxel, and C. L. Rountree, *J. Non-Cryst. Solids*, **417–418**, Nos. 1–15: 66 (2015); https://doi.org/10.1016/j.jnoncrysol.2015.02.005
17. H. Wang, P. Pallav, G. Isgrò, and A. J. Feilzer, *Dent. Mater.*, **23**, No. 7: 905 (2007); doi:10.1016/j.dental.2006.06.033
18. J. J. Kruzic, D. K. Kim, K. J. Koester, and R. O. Ritchie, *Journal of the Mechanical Behavior of Biomedical Materials*, **2**, No. 4: 384 (2009); doi:10.1016/j.jmbbm.2008.10.008
19. G. R. Anstis, P. Chantikul, B. R. Lawn, and D. B. Marshall, *Journal of the American Ceramic Society*, **64**, No. 9: 533 (1981).
20. R. F. Cook and G. M. Pharr, *Journal of The American Ceramic Society*, **73**, No. 4: 787 (1990); https://doi.org/10.1111/j.1151-2916.1990.tb05119.x
21. M. Tiegel, R. Hosseinabadi, S. Kuhn, and A. Herrmann, *Ceram. Int.*, **41**, No. 6: 7267 (2015); https://doi.org/10.1016/j.jnoncrysol.2021.120985
22. P. Lemaitre and R. Piller, *Journal of Materials Science Letters*, **7**: 772 (1988).
23. M. A. Aswad and T. J. Marrow, *Engineering Fracture Mechanics*, **95**: 29 (2012); doi:10.1016/j.engfracmech.2012.08.005
24. A. J. Mohammed, M. A. Aswad, and H. K. Rashed, *Journal of Engineering and Applied Science*, **12**, No. 6: 7935 (2017); doi:10.3923/jeasci.2017.7935.7943
25. M. A. Aswad, S. H. Awad, and A. H. Kaayem, *Journal of Mechanical Engineering Research and Developments*, **43**, No. 2: 196 (2020); jmerd.net/02-2020-196-206